TITLE

Modeling and experimental determination of infection bottleneck and within-host dynamics of a soil-borne bacterial plant pathogen.

AUTHORS

Gaofei Jiang[1, 2, #], Rémi Peyraud[2, #], Philippe Remigi[3], Alice Guidot[2], Wei Ding[1], Stéphane Genin [2] and Nemo Peeters[2*]

ORCIDs:

GJ: 0000-0002-5331-739X

RP: 0000-0002-7580-042X

PR: 0000-0001-9023-3788

AG: 0000-0001-5282-4157

WD: 0000-0001-8536-5233

SG: 0000-0003-2498-2400

NP: 0000-0002-1802-0769

AUTHOR AFFILIATION

1-Laboratory of Natural Products Pesticide, College of Plant Protection, Southwest University, Chongqing, China.

2-LIPM, Université de Toulouse, INRA, CNRS, Castanet-Tolosan, France

3-New Zealand Institute for Advanced Study, Massey University, Auckland, New Zealand.

Tel: (33) 5 61 28 55 92; Fax: (33) 5 61 28 54 61.

# Contributed equally to this work

CORRESPONDING AUTHOR

Nemo.Peeters@toulouse.inra.fr

KEYWORDS

Infection founding population, bottleneck, population dynamics; modelling; Tomato; *Ralstonia solanacearum* species complex; bacterial wilt; host-microbe interaction

ABSTRACT (250 words)

The soil is known to be a very microbe-rich environement. Plant roots are surrounded by a complex microbiota among which, in warm climates, the pathogenic bacteria belonging to the *Ralstonia sp.* species complex. We used a combination of mathematical modelling and experimental plant infection methods, mimicking the natural conditions, to define the key parameters describing the infection, colonization and wilting of the host plant ("bacterial wilt" disease). Importantly, our model takes into account the possibility for the orthologous re-infection of already infected plants. We showed that it is the case in our experimental setup and likely to also happen *in natura*. We were able to model and experimentaly measure the plant infection bottleneck, under these non-forced infection conditions. We then quantified to what extend the plant natural barriers can restrict (up to 50 times) this bottleneck size. We also measured the importance of the bacterial main virulence determinants (type III effectors) to allowing infection, as there is a reduction of the bottleneck by 70 times when the type III arsenal is absent. We further validated the model by predicting a strain's caracteristics using only a few experimentally determined parameters. Finally the analysis of the global colonization dynamics allowed an accurate assessment of the *in planta* bacterial load triggering disease.

SIGNIFICANCE STATEMENT (120 words)

Animals and plants have a complex cohabiting microbiota. These microbes can be either beneficial or deleterious to the host. We have modeled and experimentally measured the intimate interaction between a plant host (tomato) and a pathogenic, soil-associated bacteria belonging to the *Ralstonia sp.* species complex. We were able to evaluate how many bacteria are at the origin of the infection and determine how the plant and the bacteria can impact on this bottleneck. Further within-host bacterial dynamics analysis allowed to measure at what infection stage a plant would become symptomatic. Since our experimental condition allows natural infection, as well as re-infection of already infected plants, our global infection model should prove faithfull to the *in natura* conditions.

62 INTRODUCTION

63 As sessile organisms, plants can't extract themselves from their environment. Plant's natural
64 openings (like stomata, hydathodes and root permeability) are required for the gaz and solute
65 exchange between the organism and its nutrient-providing environments (air, water and soil). At the
66 same time, these environments are populated by a diverse microbiota, representing a constant
67 source of plant inoculum of beneficial, commensal but also pathogenic microbes. Roots are
68 particularly exposed as soil is known to be the most microbe-rich environment (1).

69 Not all pathogenic microbes present in a given environment will lead to a successfull plant
70 infection. Indeed infection and further colonization is dependent on the pathogen (*e.g.* virulence
71 arsenal), the host (*e.g.* developmental and immunity traits) and the environmental conditions (*e.g.*
72 temperature, hygrometry), as well as on the interactions between these parameters. These
73 constraints that sharply limit the infecting population size create bottlenecks that will drastically
74 influence population dynamics and the evolution of plant pathogens (2). Indeed, the bacterial
75 genotypes that found the infecting population in the host plant (i.e. the founders) will determine the
76 genetic makeup of subsequent generations within the host and also of future infections. A reduction
77 in genetic variability is likely to create a founder effect within the post-bottleneck population (2).
78 Moreover, plants are in constant interaction with the microbiota community, source of the pathogen
79 population in their environment. This is especially true for plant roots, in close contact with the
80 abundant soil microbiota, thus likely to face re-infections (*i.e.* homologous microbial infection) or
81 superinfection (heterologous microbial infection) (3).

82 Infection bottlenecks have been evaluated by different means in several host-microbe
83 systems. The methodologies used range from the analysis post-infection of a few marked quasi-
84 species (4, 5), several wild-type isogenic tagged strains or WITS (6), or large sequence tag-based
85 barcoded population (7). Increasing the number of tags is particularly suited for animal infection
86 systems, as fewer individuals are needed. None of these studies, aiming at quantifying infection
87 lbottlenecks, actually use natural infection routes by exposing the individual hosts to an infectious

88 microbiota. Another layer of complexity comes from the dynamics of bacterial populations within the
89 host. A global, quantitative analysis of the series of events occurring from infection to colonization
90 and ideally to dissemination is currently lacking for most host-microbial pathogens systems (3). The
91 exact assesment of all these parameters and their interactions should allow to identify the key
92 parameters of an infection and understand their influence on population structure of pathogenic
93 agents (8). Furthermore the botteleck prediction and experimental determination was performed
94 under non-forced, natural infection condition, including the possibility of subsequent re-infection.

95 Here, we quantified specific and key parameters of a plant pathogenic interaction using a
96 disease modeling approach and then, predict and experimental measured the size of the infection
97 bottleneck (or number of founders) of the pathogen. This work was conducted on the model
98 bacterial soil-borne plant pathogen *Ralstonia sp.* to understand the global parameters of plant
99 infection and colonization by a soil-borne pathogen **(9)**. This bacterium infect its hosts through the
100 roots and furthermore it is possible to complete its full life cycle in a reasonable amount of time:
101 from a soil inoculation mimicking a natural infection to complete wilting and decay of the host plant
102 (tomato) takes less than 2 weeks. In this work, we relied on this simple infection procedure followed
103 by disease scoring and bacterial load measurements to model the whole life cycle of the pathogen.
104 To our knowledge, our study is the first that provides a global modeling of the within-host population
105 dynamics for a plant bacterial pathogen. Furthermore the bottleneck prediction and experimental
106 determination was performed under non-forced, natural infection condition, including the possibility
107 of subsequent re-infection.

108 **RESULTS**

109 **Infection process modeling reveals multiple factors shaping the infection bottleneck size.**

110 The life cycle of pathogenic *Ralstonia sp.* in host plant can be divided in five subsequent steps (Fig. 1):
111 1) root invasion, 2) passage through the root cortex, 3) proliferation within the xylem vessels, 4) a
112 phenotypic switch, inducing exopolysaccharide (EPS) production, and 5) wilting of aerial organs

113 leading to the killing of the plant and allowing pathogen transmission to the soil. In order to identify
114 how those steps influence the infection founders (F) upon a prolonged exposure of the plant to the
115 pathogen (allowing susequent re-infection events (3)), we designed a mathematical model that
116 reproduces the bacterial population (B) dynamics upon these 5 steps (See SI Appendix, Method S1,
117 for the details of this model). We investigated the impact of the model parameters on the infection
118 bottleneck size of *Ralstonia pseudosolanacearum* strain GMI1000. Five of these parameters lead to a
119 reduction of the amount of founders when their value increased. These parameters are: i) the plant-
120 pathogen association constant (K, Fig. 2A), ii) the reduction of the maximum entry flow over time (z,
121 Fig. 2C), iii) the growth rate in xylem (μ, Fig. 2D), iv) the quorum sensing threshold (Q, Fig. 2E), and v)
122 the steepness of plant wilting response to EPS concentration (α, Fig. 2F).

123 Overall, the number of founders is determined by a trade-off between bacterial entry flow
124 into the roots (controlled by K, V_{fmax} and z) and the wilting kinetics (controlled by μ, Q and α). For K
125 and z the decrease of the number of founders is due to a reduction of an effective entry flow of cells.
126 On the other hand increasing parameters μ, Q and α, leads to a delayed transmission phase and thus
127 reducing the amount of bacteria entering from subsequent re-infections. However, the maximum
128 number of successful founders can dramatically increase the final founder flow value (V_{fmax}, Fig. 2B).
129 Interestingly, this last parameter represents the strength of the plant bottlenecks, *i.e.* the plant
130 barrier and the immune system clearance. Hence, we identified that the strength of these two
131 blottlenecks can represent the highest sources of founders' variability even if the within-host
132 population dynamics also plays a role.

133

134 **Experimental quantification of key parameters of the tomato infection by *Ralstonia***
135 ***pseudosolanacearum* strain GMI1000**

136 We sought to experimentally determine the values of the key parameters mentioned above in order
137 to quantitatively predict the size of the infection bottleneck. We hypothesized that plants could be

138 re-infected by the soil-inoculated pathogen. To test this in tomato, we performed non-simultaneous
139 inoculations with two equally virulent strains (SI Appendix, Fig. S1A) of *R. pseudosolanacearum*, the
140 wild type strain GMI1000 and the gentamicin-resistant derivative GRS540 (SI Appendix, Fig. S2A).
141 Tomato plants were soil-inoculated with GMI1000 and re-infected with GRS540 at 1, 8, 23 and 48
142 hours after the first inoculation (hours post-infection or hpi). Check the presence of GRS540 in the
143 bacterial load at 5 dpi showed that 60% of the plants had been re-infected when the second
144 inoculation occurred at 23 hpi. Only few re-infections were detected at 48 hpi. Hence, the capacity of
145 subsequent infection decreased over time at a rate of 2 ± 0.1 % h^{-1} (Fig. 3A).

146 Next, the median infection dose (MID) of *R. pseudosolanacearum* was quantified to evaluate
147 the infectivity of *R. pseudosolanacearum* in tomato (Fig. 3B) using the method of Reed and Muench
148 (10). The MID corresponds to the bacterial inoculums that trigger disease for, at least 50%, of the
149 inoculated plants (SI Appendix, Fig. S3). The MID gradually declined until 10 dpi to an asymptotic
150 value of $5.9 \cdot 10^6$ cells (Fig. 3B). To ensure that the MID is a feature of the soil-root interface, we
151 performed a similar assay but using stem injection to bypass the roots (SI Appendix, Fig. S4). Here,
152 the MID_{stem} was only 4.1 10^3 bacteria at 5 dpi (SI Appendix, Fig. S4D).

153 In order to evaluate bacterial growth rate in the stem, the bacterial load in infected plants
154 was quantified at different times following root infection (Fig. 4A). Fitting data points between days 2
155 and 5 yielded an exponential growth rate of 0.196 h^{-1} ± 0.039 (R^2 = 0.42) (SI Appendix, Fig. 5B). The
156 weakness of the correlation coefficients results from the intrinsic variability of the timing of the first
157 infection associated with soil inoculations procedures. In order to address this, the same experiment
158 was repeated using a stem inoculation procedure. We found a growth rate at 0.233 ± 0.012 h^{-1} (R^2 =
159 0.928 ± 0.024) (Fig. 4B), which is in the range of the *in vitro* growth rate in minimal medium: 0.253 h^{-1}
160 ± 0.034 (R^2 = 0.97 ± 0.02) (SI Appendix, Fig. S5A).

161 During the above experiment (Fig. 4A), the disease index (DI) of each plant was also recorded.
162 This DI scoring uses a 0 to 4 scale representing each a quartile of total plant leaf wilting; from 25%

163 leaves wilted (DI = 1), to 100%, or complete wilting (DI = 4). Symptomatic plants (DI > 0) have a
164 bacterial load ranging from 10^8 cfu·$g_{(FW)}^{-1}$ to 10^{11} cfu·$g_{(FW)}^{-1}$ (Fig. 5A), with the notable exception of a
165 few dried-out plants that had reached DI = 4, several days before bacterial load assessment (SI
166 Appendix Fig. S6, S7). The dataset was used to identify the *in planta* bacterial threshold triggering
167 plant symptoms. We used a two class classifier, predicting wilting onset (DI > 0) or not if the bacterial
168 load exceed a threshold (q) and compared the predictor performance in experimental value for
169 various threshold levels. The Matthews correlation coefficient (MCC) (11), which is a measure of the
170 quality of a predictor, was used to find the best threshold value. A maximum MCC value of 0.896 was
171 obtained (SI Appendix, Fig. S8) for a bacterial threshold of $6.10^7 \pm 0.97.10^7$ cfu·$g_{(FW)}^{-1}$.

172 We further exploited this large data set of more than 500 individual infected plants scored
173 for bacterial load and symptoms to extrapolate the wilting time response to the EPS production in
174 tomato plants. For this purpose, all wilting kinetics of diseased individuals were synchronised to the
175 first day when wilting symptoms were observed (Fig. 5B). The steepness, α, of the fitted wilting time
176 response curve was: 0.612 ± 0.012. Then, we determined using the equation 4 the *in planta* EPS
177 concentration from the known flux of EPS production, V_{EPS}, of *R. pseudosolanacearum* (Peyraud *et al.*
178 submitted) and the measured bacterial load and growth rate. This EPS concentration over time was
179 used to assign the scalling factor, β = 2.31, to obtain the wilting dose response curve to the EPS
180 concentration.

181 Finally, we determined the reduction of the proliferation, μ^-, due to the collapse of the host
182 tissues at late infection. From measured data of advanced wilting symptoms and bacterial load we
183 fitted a value of 0.25 h^{-1}.

184

185 **Prediction and experimental measurement of the infection bottleneck size for *Ralstonia***
186 ***pseudosolanacearum* strain GMI1000**

187 The above experimentally defined parameters, namely $K = 5.9 \cdot 10^6$, $z = 0.02$, $\mu = 0.23$,
188 $q = 6.10^7$, $\alpha = 2.31$, $\beta = 0.612$ and $\mu^- = 0.25$, were used as input in the mathematical model in order to
189 predict the size of the infection bottleneck for *R. pseudosolanacearum* strain. First we estimated the
190 maximum effective entry flow of founders, V_{fmax}, from fitting the model prediction to experimental
191 wilting onset data (extracted from Fig. 4A data). We found V_{fmax} to be in the range of 5 to 22 cells·h^{-1}.
192 The model predicts that the actual number of founders at 7 dpi should be in the range of 90 to 476
193 for an innoculum at 5.10^7 cell·ml^{-1}.

194 We then experimentally determined the size of the infection bottleneck, i.e. the number of
195 founders (N_i) in tomato using a simple statistical method based on the co-infection of GMI1000
196 mixed with minute fractions (from 1% to less than 0,1%) of the gentamycin-marked strain GRS540.
197 Importantly, both strains were shown to be of equal fitness *in planta* (SI Appendix, Fig. S1). The
198 probability of an infected plant to also contain the marked strain is directely correlated with the
199 proportion of the marked strain in the original inoculum ($p < 1\%$, see Materials and methods) and the
200 size (N_i) of the infection bottleneck. Sets of 32 plants were inoculated with a given GMI1000/GRS540
201 ratio (p). The resulting proportion of plants infected by GRS540 was then used to generate a single
202 estimation of N_i through a probabilistic analysis (see M&M and SI Appendix, Fig. S9). After extensive,
203 60 independent inoculations of sets of 32 plants, the median of N_i was estimated to be 458 cells (SI
204 Appendix Fig. S10). We observed a high variability of N_i with a two times standard deviation of 2734
205 cells. This variability could reflect the true biological variability of N_i, however it may also arise from
206 the stochastic sampling of the marked strain inherent to our experimental setup. Thus, in order to
207 evaluate the contribution of a stochastic sampling of the marked strain on N_i variation, we simulated
208 a random sampling based on the same parameters as the experimental setup (number of plants,
209 concentration of marked strain in innoculum). For a true *Ni* value of 458 the stochasticity analysis
210 gave a median N_i of 454 cells (SI Appendix Fig. S10), with a two times standard deviation of 507 cells.
211 Hence, we evaluated that the stochasticity of individual sampling due to our experimental setup
212 could represent up to 18% (507/2734) of the variability observed in the experimental N_i estimation.

213

214 **Plant physical barriers and pathogen type III effectors are major drivers of the infection bottleneck**
215 **size.**

216 We used a wounded-root inoculation procedure to estimate the contribution of plant natural
217 root barriers to the infection bottleneck size. At 4 dpi, all wounded-root plants had symptoms,
218 indicating an accelerated infection and colonization. We used the same methodology of mixed
219 inoculations to determine the impact of wouding on the infection bottleneck size ($N_{WT\text{-}wounding}$). We
220 were able to show that $N_{\text{WT-wouding}}$ dramatically increased to a median of 24215 cells (Fig. 7, blue
221 circles), significantly larger than N_{WT} (median of 458 cells) as previously defined (Mann Whitney test,
222 P-value < 0.0001). Analysis of variation in model parameters which fits such high N_i values and
223 earliest symptoms onset (4 days), reveals that a high entry flow, V_{fmax}, around 1065 cells·h^{-1} likely
224 occurred in addition to the reduction of the delay time, d, to cross root cortex.

225 We then treated tomato plants with an *hrp* mutant (*R. pseudosolanacearum* strain GMI1694*,*
226 *hrcV* mutant) and its isogenic gentamycin-marked strain (GRS743, SI Appendix Fig. S1B*),* to evaluate
227 the impact of a complete loss of bacterial type III secretion on the infection bottleneck size. Tomato
228 plants were harvested at 10 dpi in order to maximize the colonization of plants by the *hrp* defective
229 *R. pseudosolanacearum* strain. Here, the infection bottleneck size of the *hrp* mutant, N_{hrp}, was
230 estimated at a median of 6 cells (and mean of 7 ± 4 cells, Fig. 7, green squares), significantly lower
231 than N_{WT} (Mann Whitney test, P-value = 0.0014).

232

233 **Using the model to infer life-history traits of a bacterial mutant**

234 The results obtained so far indicated that our model is able to correctly predict the size of the
235 infection bottleneck from a few key parameters that were determined experimentally. We wondered
236 if the model could be used with the opposite goal, *i.e.* inferring a strain's characteristics from a
237 measured number of founders. In *R. pseudosolanacearum,* the type III secretion system (or TTSS) is

238 required for bacteria to enter xylem vessels (12). A mutant in the TTSS apparatus (*hrp* mutant) is
239 unable to kill plants, but can sustain a limited population sizes in xylem vessels (13).

240 We therefore combined the wounding procedure and the inoculation with the *hrp* strains. Samples
241 were harvested to estimate the number of founders of a *hrp* mutant by wounding ($N_{hrp_wounding}$) at 7
242 dpi. The founder amount increased to a mean of 62 ± 40 cells and a median of 53 cells. The mean of
243 $N_{hrp_wounding}$ was about 9 times higher than N_{hrp} (P-value = 0.019) but 482 times lower than $N_{WT_wounding}$
244 (P-value = 0.0006).

245 We used these data to infer the strength of the immune system clearance on the entering
246 bacterial cells and the *in planta* growth rate for GMI1694. The entry flow of founders, $V_{fmax(hrp_wounding)}$,
247 was estimated to be around 3 cells·h^{-1}. Thus, if considering that the entry flow in wounded roots of
248 the *hrp* mutant is similar to the wt (1065 cells·h^{-1}) and that the succesfull founder flow corresponds
249 to the survivors to the immune system response, we found that the strength of the immune system
250 clearance was 99.7% of the entered cells. Comparison between the founding number of the wt, 458,
251 and the *hrp* mutant strain, around 6, leads to a similar value, 98.7 %. Then, we estimated the
252 maximal growth rate of GMI1694 by considering that no symptoms occurs and thus bacterial load
253 remains below the quorum sensing treshold, q, for both intact and wounded root conditions. We
254 found that the maximal growth rate *in planta* should be in the range of 0.9 to 0.11 h^{-1}. We
255 experimentally tested this prediction by measuring the growth rate of the GMI1694 strain in stem
256 xylem using the stem injection procedure (SI Appendix, Fig. S11) and found a growth rate of 0.112 ±
257 0.005 h^{-1}, with R^2= 0.873 ± 0.06. Hence, the clearance of the *hrp* mutant bacteria by the plant
258 immune system in the stem was evaluated to be at a maximum of 52 %.

259

260 **DISCUSSION**

261 Our objective in this work was (i) to model the plant infection process and the within-host bacterial
262 population dynamics, (ii) predict and experimental measure the infection bottleneck size for
263 *R. pseudosolanacearum* strain GMI1000 on tomato and finally, (iii) to understand the factors that
264 participate to the bacterial infection bottleneck. For this purpose we used a natural, soil-drenching,
265 plant infection bioassays. Plants were scored for disease appearance (bacterial wilt) and bacterial
266 load. The lowest level of bacterial soil saturation to obtain reliable wilting (> 50%) in our conditions
267 (12 days), is asymptotic to a value of 6.10^6 cfu·ml^{-1} of inoculum (see Fig. 3B). In our experimental
268 setup this equates to a 4.6 10^6 cfu·g^{-1} Dry Weight soil inoculum, comparable to the 10^5 -10^7 cfu·g^{-1} Dry
269 Weight of soil detected in the rhizosphere of diseased tomato plants in the field (14). We also
270 showed that there is a potential for subsequent re-infection, over a time frame of 24-48 h (see Fig.
271 3A). The success of these further re-infections is likely to be dependent on the density of the local
272 inoculums which can decline other time (15) and on the interaction between the host immune
273 response and the bacterial virulence arsenal. Indeed, the lowering of the re-infection probability with
274 time (see Fig. 3A) could be correlated with the onset of plant immune responses (13).

275 We showed (Fig. 5A) that asymptomatic plants are displaying different levels of bacterial colonization
276 whereas diseased plants are always well colonized (>10^8 cfu/gFW). We further refined this
277 relationship by analyzing the large data set of individual plants for which we have obtained both the
278 disease score and the bacterial count. We were able to determine the *in planta* bacterial load
279 (6.10^7Cfu/g FW) that would be the best predictor of later wilting (see SI Appendix, Fig. S8). As
280 *Ralstonia sp.* plant pathogenic strains are restricted to the xylem vessels of plants, representing
281 probably less than a 1/10 of the volume/weight of a stem, we could consider our *in planta*
282 experimental validation as being in the same range as the threshold (10^7-10^8 cfu/ml) determined to
283 trigger EPS production *in vitro* **(16)**.

284 In order to understand and determine all the important parameters of the life cycle of pathogenic
285 *Ralstonia sp.,* we built a model that captures the global life cycle of the bacterium from infection to
286 dissemination in the environment after complete wilting of the host plant. We experimentally
287 estimated the size of the infection bottleneck (*i.e.* the number of founders) by a probabilistic
288 approach evaluating the presence/absence of a marked strain in the colonized plants at the earliest
289 stage possible. This experimentally determined number of founders (median N_i =458 cells) was
290 obtained after the analysis of a large number of individual plants and is in the same range as the one
291 predicted from the model (N_i = 90 to 476). To our knowledge, it is the first determination of the host-
292 bacterial pathogen infection bottleneck that takes into account re-infection in an experimental
293 system mimicking natural infection.

294 The quantification of this bottleneck imposed by the plant on the bacterial population present in the
295 soil is required to evaluate the possibility of a "founder effect". This latter is defined as a bottleneck
296 too narrow to allow the genetic diversity of the infecting population to mirror the genetic diversity of
297 the soil resident population, leading to a potential genetic drift. The *Ralstonia solanacearum* Species
298 Complex (RSSC) has a wide species-to-continent geographic distribution **(17)**. Some studies show that
299 diversity analysis of single isolates from different infected plants can yield up to 42-51 haplotypes
300 mainly from 2 RSSC species (*R. solanacearum* and *R. pseudosolanacearum* formerly defined as
301 phylotypes II and I **(17)**) over a narrow geographical distribution **(18, 19)**. So far no studies have
302 explored the RSSC population diversity in the soil of planted fields, thus it is not possible to establish
303 whether the size of the infection bottleneck as determined in this work for the GMI1000 strain would
304 *per se* result in a genetic drift or not. In addition, in this study, the infection bottleneck was measured
305 using a clonal population (individuals of the same clone, GMI1000 and isogenic marked strain).
306 However, in a local natural population, different bacterial genotypes could also contribute to the
307 infection bottleneck size (*i.e.* presence of strains with different virulence arsenals, different
308 metabolic capacities). Studying the contribution of different bacterial genotypes to the infection
309 bottleneck size would be an interesting question for future studies. An interesting corollary of

310 bottleneck restriction during infection is related to kin selection. Indeed one could imagine that the
311 restriction imposed by the bottleneck will prevent (or reduce) the infection by non-kin bacteria. This
312 would limit the super-infection by opportunistic microbes or re-infection by kin-cheaters, generating
313 a highly related infecting population **(3, 20)**. Studying the ability of different bacterial genotypes to
314 alter bottleneck sizes in isolation or within diverse (multi-strain or multi-species) communities
315 will/would be an interesting question for future studies.

316 In this study we also evaluated the effect of plant and bacterial parameters on the size of the
317 infection bottleneck. As expected, the bottleneck size increased significantly (> 50 times) after
318 mechanically wounding the roots. We also showed that this bottleneck was dramatically reduced
319 (> 70 times), when plants were infected with a *hrp* mutant, devoid of any type III effectors, and
320 known to produce symptomless but colonized plants **(13)**. This later result shows that type III
321 effectors are collectively required to establish the first infecting front, like previously shown for
322 specific type III effectors in an *in vitro* infection model **(21, 22)**. We can hypothesize that one of the
323 prevalent role of these virulence determinants would be to suppress plant immunity, but we can't
324 rule out their role in nutrient mobilization, even at these early infection stages. Finally, we tested the
325 prediction power of our global infection model by testing the predicted *in planta* growth rate of the
326 *hrp* mutant strain when inoculated on wounded plants. As the experimentally measured growth rate
327 fits with the predicted maximal growth rate, our starting hypothesis of same entry flow (in wounded-
328 root plants) but greater clearance of the *hrp* mutant bacteria by the plant immune system holds true.

329 Several important questions are still unresolved regarding the parameters controlling the size of the
330 infection bottleneck **(2)** during the infection of tomato plants by *Ralstonia sp.* In particular it would
331 be interesting to evaluate variation in the infection bottleneck size with the plant root status, both in
332 term of root growth (young *vs* old plants) and in terms of root developmental plasticity (*e.g.* in
333 different type of soils). At a smaller scale even, one could imagine that there could be specific
334 bottelnecks for the bacteria to cross several distinct cell layers within the root organ **(12)**, like it was
335 shown for the progression of the anthrax bacteria in different murine tissues **(4)**. Another level of

complexity would be to understand the contribution of the microbiome to this bottleneck. Specifically, it would be interesting to evaluate whether the protection of plants from bacterial wilt by trophic competition **(15)** could partly be explained by an “infection-site crowding” thus inducing a likely reduction in the infection bottleneck size.

343 **MATERIAL AND METHODS**

344 **Infection model**

345 We designed a mathematical model of the infection kinetics to describe the population
346 dynamics of *R. pseudosolanacearum* and the founder number within the xylem. The model is
347 composed of 3 compartments (c), the soil (s), the root cortex (r), and the xylem (x). The volume
348 dimention of the model was set in ml, since it corresponds to the concentration of cells using soil
349 drenching methods, and the bacterial load measured in g (fresh weight) wich can be assumed to be
350 in the range of 1 ml volume. The variables are the concentration of the bacterial cells B_c within the 3
351 compartments (in cell·ml^{-1}), the fouder number, F, in the root cortex, F_r, and xylem, F_x, (in cell·ml^{-1}),
352 the EPS concentration in xylem, EPS_x, (in mmol·ml^{-1} of N-acetylglucosamine), the wilting level of the
353 plant, W, (in DI). B and F can be in the magnitude of few cells in tissues, thus we used entier value for
354 these variables. The equations, described in the supplementary information, are solved numerically
355 with a time step of 1 hour. The transmission time was defined as the time when the wilting symptom
356 reaches DI > 3.5. When no wilting level above 3.5 is reached after 30 days, this time point is taken for
357 the evaluation of the infection bottleneck.

358 **Bacterial strains, plant material and culture conditions**

359 The *R. pseudosolanacearum* strains used in this work were: GMI1000, the wild-type strain; GRS540, a
360 derivative strain from GMI1000 with a gentamicin cassette insertion (23); GMI1694, a type III
361 secretion system mutant (*hrcV* mutant) with spectinomycin cassette insertion (24); GRS743, a
362 derivative strain from GMI1694 with the integration of the gentamicin cassette of GRS540 (this
363 study). The gentamicin cassette does not alter the pathogen fitness, as was previously shown by
364 stem injection (23) and SI Appendix, Fig. S1. *R. pseudosolanacearum* strains were routinely grown at
365 28 °C in complete BG medium (25). Antibiotics were used at the following final concentrations: 10
366 µg·L^{-1} gentamicin and 40 µg·L^{-1} spectinomycin. *Solanum lycopersicum* var. Super Marmande was
367 cultivated in greenhouse. Square trays (30×30×4.5 cm) were used to grow 16 tomato seedlings and

368 kept in the greenhouse under the following conditions: 75% humidity, 12 h light 28 °C, and 12 h
369 darkness 27 °C. Plants were inoculated after 4 weeks of growth in dedicated quarantine facilities.

370 **Determination of the median infection dose**

371 Wild-type *R. pseudosolanacearum* GMI1000 was used to determinate the median infection dose
372 (MID) in tomato. Groups of 16 tomato plants in one tray were soil-drenching inoculated with 5.10^8,
373 5.10^7, 5.10^6, 5.10^5 or 5.10^4 cfu·ml^{-1} in 500 ml of bacterial suspension. For stem injection, 10 µl of
374 bacterial suspensions was directly injected into stem with a microsyringe (Hamilton, Reno, NV,
375 U.S.A.) at the level of the cotyledon. The injection inoculums were diluted to 5.10^7, 5.10^6, 5.10^5, 5.10^4
376 and 5.10^3 cfu·ml^{-1} of *R. pseudosolanacearum*. Symptom appearance was scored daily for each plant.
377 Disease index (DI) was used to describe the observed wilting: 0 for no wilting; 1 for 25% of leaves
378 wilted; 2 for 50%; 3 for 75% and 4 for complete wilting. Symptom onset (DI > 0) was defined as an
379 infection success of *R. pseudosolanacearum* in tomato. The MID of *R. pseudosolanacearum* in tomato
380 was used at the 50% endpoint method of Reed and Muench (10). First, we calculated the Reed and
381 Muench index (RMI) for the 50% endpoint from these dilutions. The obtained RMI was then
382 corrected by the dilution factor.

383 $$RMI = \frac{(\%\ infected\ at\ dilution\ inmmediately\ above\ 50\%) - 50\%}{(\%\ infected\ at\ dilution\ inmmediately\ above\ 50\%) - (\%\ infected\ at\ dilution\ inmmediately\ below\ 50\%)}.$$

384 $$Logarithm\ of\ MID = (\text{logarithm of the dilution above 50\% infection}) + \text{RMI} \times \text{dilution factor}.$$

385 Each treatment had two technical repeats and three biological repeats with 96 plants in total.

386 **Monitoring of bacterial colonization kinetics and *in planta* growth rate.**

387 The soil-drenching inoculation was performed using GMI1000 at 5.10^7 cfu·ml^{-1}. Symptoms were
388 recorded before harvest as described above. Sixteen plants were sampled at each dpi and this
389 experiment was repeated three times with 48 samples in total. For the stem injection procedure,
390 each plant was injected with 10 µl bacterial solution containing 5.10^6 cfu·ml^{-1} of GMI1000. Sampling
391 was conducted straight away after injection (0hpi), 7 hpi, 24 hpi and 52 hpi. Each sampling had 4
392 plants and this experiment was repeated 8 times with 32 samples in total. The 1 cm stem from the

393 cotyledons upwards was harvested, weighed, and homogenized by mechanical disruption in a
394 grinder (Retsch France, 95610 Eragny sur Oise, France). Bacteria were then enumerated by plating
395 serial dilutions on BG agar plates, using an easyspiral (Interscience, Saint Nom la Breteche, France).

396 **Prediction of bacterial threshold to induce symptom.**

397 The following relation was used to predict wilting onset W (W=1) or no witling (W=0) depending on
398 the bacterial load b, in cfu·ml^{-1}, *in planta*.

399 W = 1 if b > t then W = 0

400 With t, the threshold above which the wilting onset occurs. Two-class contingence matrices
401 with experimental and simulated data were generated for changing values of t. The Matthews
402 Correlation Coefficient (11) (MCC) was used to compare predicting capacities of t. The MCC can
403 range from 0 (random assignment) to 1 (perfect prediction).

404 **Estimation of the size of the infection founding population (N_i)**

405 A method was developed to quantitatively estimate the size of the *R. pseudosolanacearum*
406 infection founding population in tomato, or N_i. The method is based on the measurement of the
407 proportion of plants infected with a gentamycine marked strain when the host was inoculated with a
408 mixture of two strains, the wt strain plus various small (0.1% to 0.01%) proportion of a marked strain.
409 The starting frequency of the marker strain in the inoculum, *p*, was measured by serial plating. The
410 frequency of the wt strain being 1 - *p*. R is referred to as the event that at least one cell of the
411 resistant bacteria individual is present in the host plant. *P*(*R*) is the probability of the event R. NR is
412 considered as the event that only the wt (Non-Resistant) strain is present. *P*(*NR*) is the probability of
413 the event NR. Thus, $P(R)+P(NR)=1$. Based on the above: $P(NR) = (1 - p)^{Ni}$ and $P(R)=1 - (1 - p)^{Ni}$. And
414 $N_i = \log(1 - P(R)) / \log(1 - p)$. SI Appendix, Fig. S9 highlights the sigmoid feature of N =f(P) for each
415 given *p*.. N_i, or "infection bottleneck" can be estimated from this expression through investigating
416 *P*(*R*) experimentally as follows: The resistant, marked strains are GRS540 or GRS743, and their
417 respective non-marked isogenic strains are GMI1000 and GMI1694 (*hrp* mutant). The sampling time

418 was at 7 dpi for root inoculation of GMI1000 and GRS540, 4 dpi for wounding inoculation of GMI1000
419 and GRS540, 10 dpi for inoculation of GMI1694 and GRS743 and 7 dpi for wounding inoculation of
420 GMI1694 and GRS743. Stem samples were collected as described before and appearance of the two
421 strains was determined by plating on BG agar with and without antibiotics. The two extreme output
422 value of N_i, *i.e.* N_i= 0 and N_i= infinity, respectively obtained when *P(R)*= 0/32 or *P(R)*= 32/32 were
423 excluded from the analysis as they artificially skew the estimation of N_i. Indeed these limit values are
424 the two asymptotes of the sigmoid curve of N= f(P) (see SI Appendix Fig. S9)

425

426 ACKNOWLEDGEMENTS

427 GJ was supported by China Scholarship Council (No. [2013] 3009) and TECHNO II Erasmus Mundus
428 Programme (2015-2016). RP was supported by EMBO (Long-Term Fellowship ALTF 1627-2011) and
429 Marie Curie Actions (EMBOCOFUND2010, GA-2010-267146). This work was performed with funding
430 from the LABEX "TULIP" (ANR-10-LABX-41). We also thank our colleagues for useful discussions. The
431 funding bodies played no role in study design, data collection and analysis, decision to publish, or
432 preparation of the manuscript.

433

434 AUTHORS CONTRIBUTION

435 GJ, RP, PR and NP designed the research, GJ, RP performed research, GJ, RP, AG, SG and NP analyzed
436 data, GJ, RP, PR, AG, SG, WD and NP wrote the paper. All authors have read and approved the
437 manuscript for publication. GJ and RP contributed equally to the work.

438

439

440

441

442 **REFERENCES**

443 1. Zarraonaindia I, et al. (2015) The soil microbiome influences grapevine-associated microbiota.
444 *mBio* 6(2):e02527–14–10.

445 2. Abel S, Abel Zur Wiesch P, Davis BM, Waldor MK (2015) Analysis of Bottlenecks in
446 Experimental Models of Infection. *PLoS pathogens* 11(6):e1004823.

447 3. Gog JR, et al. (2015) Seven challenges in modeling pathogen dynamics within-host and across
448 scales. *Epidemics* 10:45–48.

449 4. Plaut RD, Kelly VK, Lee GM, Stibitz S, Merkel TJ (2012) Dissemination bottleneck in a murine
450 model of inhalational anthrax. *Infection and immunity* 80(9):3189–3193.

451 5. Pfeiffer JK, Kirkegaard K (2006) Bottleneck-mediated quasispecies restriction during spread of
452 an RNA virus from inoculation site to brain. *Proc Natl Acad Sci USA* 103(14):5520–5525.

453 6. Grant AJ, et al. (2008) Modelling within-Host Spatiotemporal Dynamics of Invasive Bacterial
454 Disease. *PLoS biology* 6(4):e74–14.

455 7. Abel S, et al. (2015) Sequence tag–based analysis of microbial population dynamics. *Nature*
456 *Methods* 12(3):223–226.

457 8. Louie A, Song KH, Hotson A, Thomas Tate A, Schneider DS (2016) How Many Parameters Does
458 It Take to Describe Disease Tolerance? *PLoS biology* 14(4):e1002435.

459 9. Peeters N, Guidot A, Vailleau F, Valls M (2013) Ralstonia solanacearum, a widespread bacterial
460 plant pathogen in the post-genomic era. *Molecular Plant Pathology* 14(7):651–662.

461 10. Reed LJ, Muench H (1938) A simple method of estimating fifty per cent endpoints. *Am J*
462 *Epidemiol* 27(3):493–497.

463 11. Matthews BW (1975) Comparison of the predicted and observed secondary structure of T4
464 phage lysozyme. *Biochimica et biophysica acta* 405(2):442–451.

465 12. Vasse J, Genin, S., Frey P, Boucher C, Brito B (2000) The hrpB and hrpG regulatory genes of
466 Ralstonia solanacearum are required for different stages of the tomato root infection process.
467 *Molecular plant-microbe interactions: MPMI* 13(3):259–267.

468 13. Feng D-X, et al. (2012) Biological control of bacterial wilt in Arabidopsis thaliana involves
469 abscissic acid signalling. *New Phytol* 194(4):1035–1045.

470 14. Horita M, Tsuchiya K (2005) Diversity of *Ralstonia solanacearum* in Tomato Rhizosphere Soil.
471 *Bacterial Wilt Disease*, eds Prior P, Allen C, Elphinstone J (Allen, C. Prior, P. Hayward, A.C.).

472 15. Wei Z, et al. (2015) Trophic network architecture of root-associated bacterial communities
473 determines pathogen invasion and plant health. *Nature communications* 6:8413.

474 16. Clough SJ, Flavier AB, Schell MA, Denny TP (1997) Differential Expression of Virulence Genes
475 and Motility in Ralstonia (Pseudomonas) solanacearum during Exponential Growth. *Applied*
476 *and Environmental Microbiology* 63(3):844–850.

477 17. Safni I, et al. (2014) Polyphasic taxonomic revision of the Ralstonia solanacearum species
478 complex: proposal to emend the descriptions of Ralstonia solanacearum and Ralstonia syzygii
479 and reclassify current R. syzygii strains as Ralstonia syzygii subsp. syzygii subsp. nov., R.
480 solanacearum phylotype IV strains as Ralstonia syzygii subsp. indonesiensis subsp. nov.,
481 banana blood disease bacterium strains as Ralstonia syzygii subsp. celebesensis subsp. nov.
482 and R. solanacearum phylotype I and III strains as Ralstonia pseudosolanacearum sp. nov. *Int J*
483 *Syst Evol Microbiol* 64(Pt 9):3087–3103.

484 18. Ramsubhag A, et al. (2012) Wide genetic diversity of Ralstonia solanacearum strains affecting
485 tomato in Trinidad, West Indies. *Plant Pathology* 61(5):844–857.

486 19. Lin CH, Tsai KC, Prior, P., Wang J-F (2014) Phylogenetic relationships and population structure
487 of Ralstonia solanacearum isolated from diverse origins in Taiwan. *Plant Pathology* 63:1395–
488 1403.

489 20. van Leeuwen E, O'Neill S, Matthews A, Raymond B (2015) Making pathogens sociable: The
490 emergence of high relatedness through limited host invisibility. *The ISME journal*.
491 doi:10.1038/ismej.2015.111.

492 21. Turner M, et al. (2009) Dissection of bacterial Wilt on Medicago truncatula revealed two type
493 III secretion system effectors acting on root infection process and disease development. *Plant*
494 *Physiology* 150(4):1713–1722.

495 22. Wang K, et al. (2015) Functional Assignment to Positively Selected Sites in the Core Type III
496 Effector RipG7 from Ralstonia solanacearum. *Molecular Plant Pathology*:n/a–n/a.

497 23. Guidot A, et al. (2014) Multihost experimental evolution of the pathogen Ralstonia
498 solanacearum unveils genes involved in adaptation to plants. *Molecular Biology and Evolution*
499 31(11):2913–2928.

500 24. Cunnac S, Occhialini A, Barberis P, Boucher C, Genin S (2004) Inventory and functional analysis
501 of the large Hrp regulon in Ralstonia solanacearum: identification of novel effector proteins
502 translocated to plant host cells through the type III secretion system. *Molecular Microbiology*
503 53(1):115–128.

504 25. Plener L, Boistard P, González A, Boucher C, Genin S (2012) Metabolic adaptation of Ralstonia
505 solanacearum during plant infection: a methionine biosynthesis case study. *PloS One*
506 7(5):e36877.

507

508

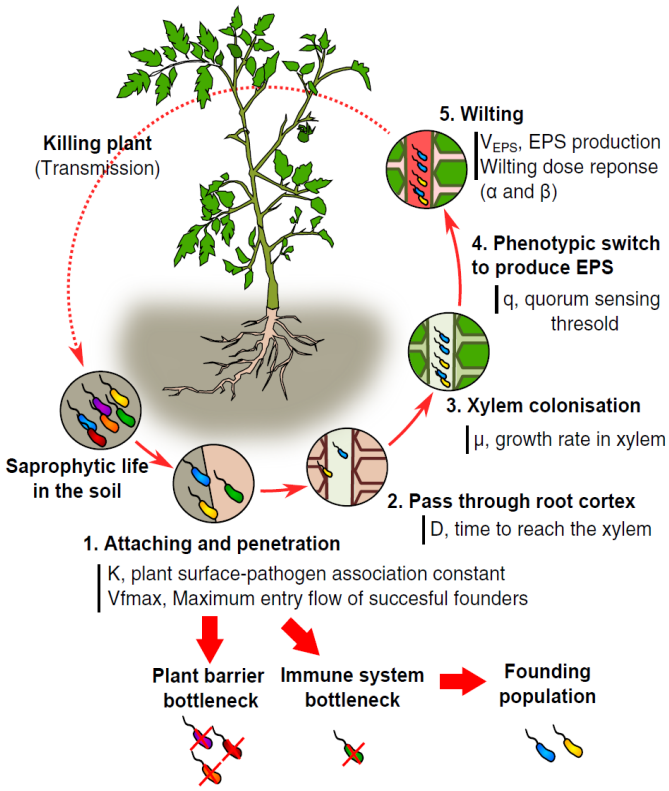

Figure 1: The life cycle of plant pathogenic *Ralstonia sp.*

Ralstonia sp. lives in the soil, penetrates into the plant through the roots, pass the root cortex and then colonize the xylem vessels. When high bacterial densities are reached, a phenotypic switch is induced with production of exopolysaccharide (EPS).The xylem water flux is interrupted, promoting the wilting symptoms. After plant death, the bacteria returns to the soil where it will continue as a saprophyte until a new host is infected.

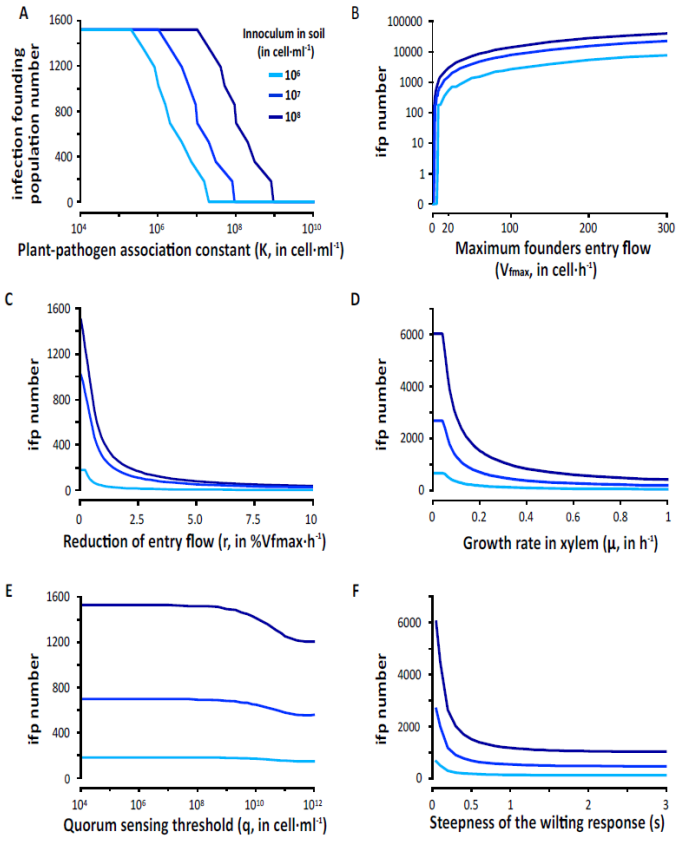

Figure 2: Sensitivity of the infection bottleneck to different parameters of the infection cycle.

Simulations were performed using the population dynamics model (see results) and by varying the different values of the model parameters K (panel A), V_{fmax} (panel B), r (panel C), µ (panel D), q (panel E), s (panel F), see the list Fig.1 and Appendix SI Fig. 2. Simulations were performed for 3 concentrations of bacterial soil inoculum, 1.10^6, 1.10^7 and 1.10^8 cell·ml^{-1}.

524

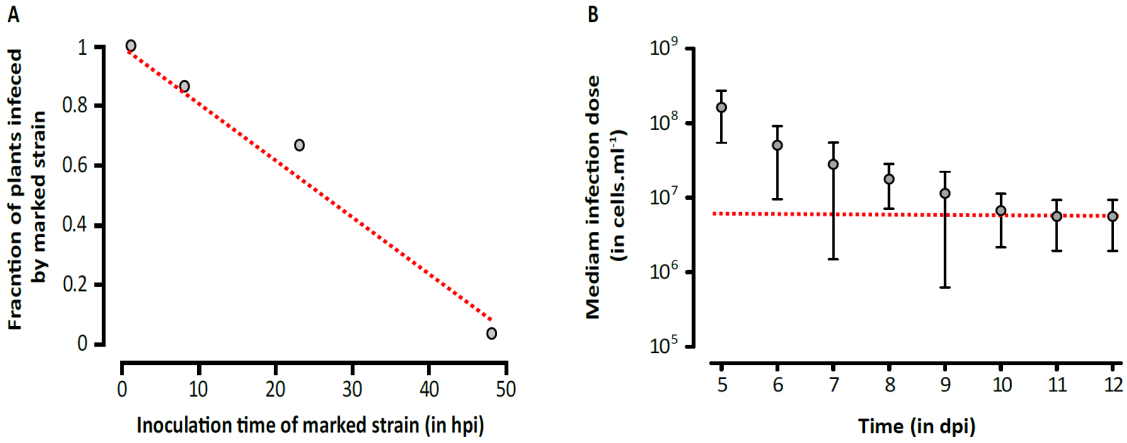

525

526 **Figure 3: Infectivity of *Ralstonia pseudosolanacearum* in tomato.**

527 (A) Tomato host is continuously infected by *R. pseudosolanacearum* within 48 hours. Plants were first
528 inoculated with the wild type GMI1000 strain and subsequently inoculated with the marked GRS540
529 strain (SI Fig. 1A) at 1, 8, 23 and 48 hours after the first inoculation. Bacterial load of these two
530 strains were quantified at 5 dpi to obtain the fraction of GRS540 in final bacterial population. (B) The
531 median infection dose (MID) of *R. pseudosolanacearum* in tomato following soil-drenching
532 inoculation. Five 10 times dilution of *R. pseudosolanacearum* inoculums, volume of 500 ml per trial,
533 were poured on each tray of 16 plants. Daily phenotyping was performed (SI Fig. 3) and the Reed-
534 Muench method was adopted to determine the MID at each dpi. The red dotted line represent an
535 asymptotic value at MID = $5.9 \cdot 10^6$ cells.

536

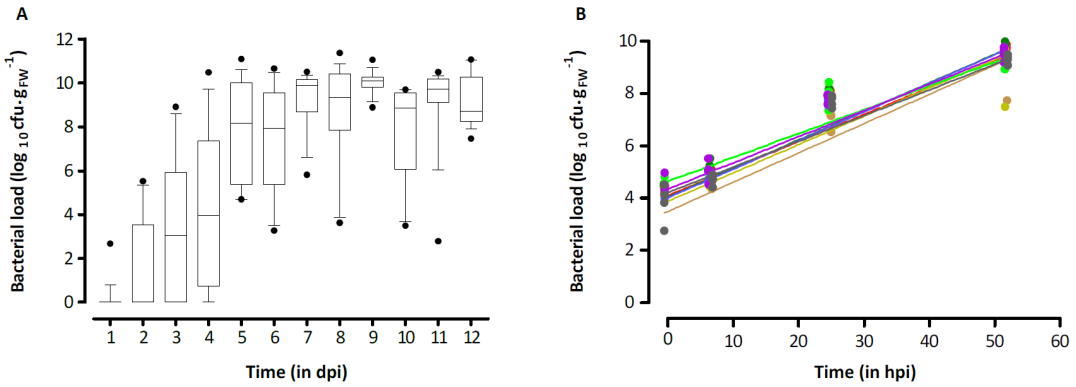

537

538 **Figure 4: Colonization dynamics of *Ralstonia pseudosolanacearum in planta*.**

539 (A) The bacterial load of individual tomato plants was assessed from 1 dpi to 12 dpi. Sixteen plants
540 were analysed at each time-point (dpi). This experiment is representative of 3 biological replicates
541 (Appendix SI Fig. 6). Bar represents the median of bacterial load in each group. (B) *In planta* growth
542 of *R. solanacearum* after the stem injection inoculation. Samples were harvested at 0, 7, 25, 52 hpi.
543 Thirthy-two individual plants from 8 biological replicates were analysed. After growth curve fitting,
544 the rate was determined at 0.233 ± 0.012 h^{-1}; R^2 = 0.937± 0.024 (mean ± sd).

545

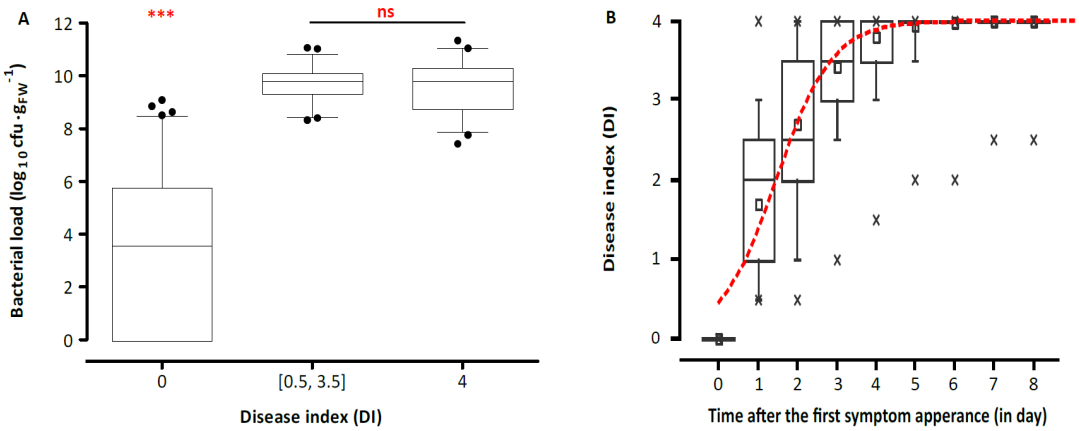

546

547 **Figure 5: Bacterial wilt disease dynamics.**

548 The data from Fig. 4A was used for this correlation analysis with three biological repeats (SI Fig. 7).
549 (A) Correlations of bacterial load and disease index (DI) in tomato. Box plots represent the median
550 and 5-95 percentiles in each DI group. *** indicates P-value < 0.0001, Mann-Whitney test, ns: P-
551 value > 0.05. (B) Time response curve of symptom onset (wilting) synchronized to the first day of the
552 symptom appearance for each individual plant.

553

554

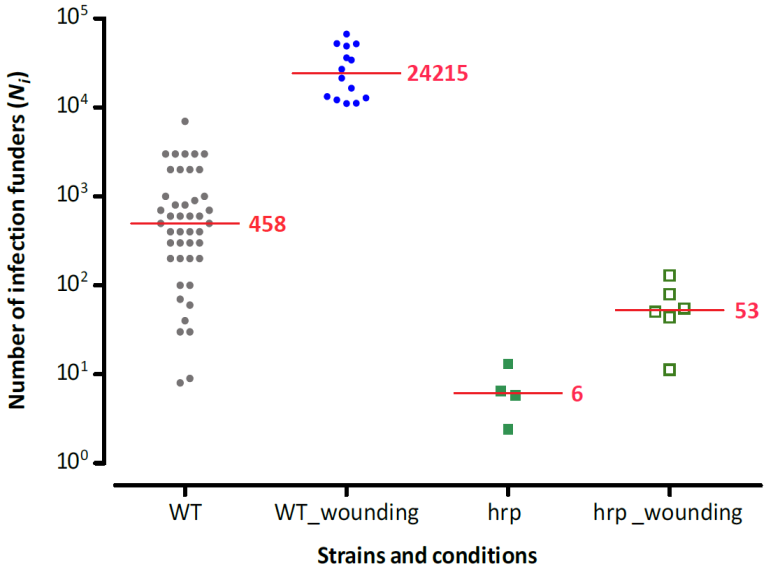

P-value	WT	WT_wounding	hrp
WT_wounding	< 0.0001		
hrp	0.0014	0.0035	
hrp_wounding	0.0032	0.0006	0.019

555

556 **Figure 6. Contribution of plant physical barriers and bacteria type III effectors to the infection**

557 **bottleneck size.**

558 Wild type GMI1000 (grey dots) and *hrp* mutant GMI1694 (hrp, green squares) of *R.*

559 *pseudosolanacearum* were harvested at 7 dpi and 10 dpi following root inoculation. GMI1000

560 wounding (WT-wounding, blue dots) and GMI1694 wounding (hrp_wounding, green open squares)

561 were harvested at 4 dpi and 7 dpi by wounding root inoculation. Each experimental condition can be

562 distinguished from the others as indicated by the Mann-Whitney test P-values in the table.

563
564
565